The Journal of Experimental Biology 202, 2371–2383 (1999)
Printed in Great Britain © The Company of Biologists Limited 1999
JEB2115

VOLTAGE-DEPENDENT IONIC CURRENTS IN THE VENTROMEDIAL ECLOSION HORMONE NEURONS OF *MANDUCA SEXTA*

RANDALL S. HEWES*

Department of Zoology, University of Washington, Seattle, Washington 98195, USA

*Present address: Department of Anatomy and Neurobiology, Box 8108, Washington University School of Medicine, 660 South Euclid Avenue, St Louis, MO 63110, USA (e-mail: hewesr@thalamus.wustl.edu)

Accepted 2 June; published on WWW 9 August 1999

Summary

The ventromedial cells (VM cells) of the moth *Manduca sexta* belong to a peptide hormone signaling hierarchy that directs an episodic and stereotyped behavior pattern, ecdysis. The VM cells respond to declining ecdysteroid titers at the end of the final larval molt with a transcription-dependent decrease in spike threshold and the abrupt release of the previously stockpiled neuropeptide, eclosion hormone (EH). This report describes whole-cell patch-clamp recordings of acutely isolated VM cell somata made to identify membrane currents that may underlie the increase in VM cell excitability during EH release and that may contribute to abrupt peptide release. There were at least three voltage- and time-dependent conductances in the VM cells. The inward current was carried exclusively by a voltage-dependent inward Ca^{2+} current (I_{Ca}), and the outward currents were a combination of a Ca^{2+}-dependent outward K^+ current ($I_{K(Ca)}$) and a transient, voltage-dependent outward K^+ current, the A current (I_A). In current-clamp recordings, the currents present in the acutely isolated somata were sufficient to generate membrane properties similar to those observed in the VM cells *in situ*. This study represents the first step toward characterization of the mechanisms underlying the abrupt release of EH stores from the VM cells preceding ecdysis.

Key words: eclosion hormone, ecdysis, *Manduca sexta*, ecdysteroid, neuropeptide, ecdysis triggering hormone, neurosecretory cell.

Introduction

All insects molt repeatedly during their life cycle to accommodate growth and the changes in external body form that occur during development and metamorphosis. After synthesis of the outer layers of the new cuticle, the inner layers of the old cuticle are digested and resorbed (Riddiford and Truman, 1978). The outer layers of the old cuticle remain and must be shed through a stereotyped series of behavior patterns collectively called ecdysis. Ecdysis is a particularly vulnerable period in the insect life cycle, since other types of behavior such as normal locomotion and grooming are generally suppressed (e.g. Carlson, 1977). At the same time, the new cuticle remains soft and pliant to allow the insect to extricate itself from the old cuticle and to allow expansion after ecdysis. Ecdysis must begin after the old cuticle is sufficiently degraded and detached, and it must be completed before portions of the new cuticle harden. Thus, ecdysis is tightly regulated, and its successful completion requires (1) precise coordination of multiple behavior patterns, developmental events and physiological changes, and (2) signaling between the epidermis, central nervous system (CNS) and other tissues (Reynolds, 1980).

These requirements are met by a complex hierarchy of endocrine and paracrine signals that have been investigated most intensively in the tobacco hornworm *Manduca sexta*. Each molt is initiated and coordinated by a large peak in the titer of circulating ecdysteroids, which directs the epidermis to synthesize the new cuticle (Riddiford and Truman, 1978). Following the ecdysteroid peak, the decline in the titer triggers digestion and resorption of the old cuticle and, ultimately, ecdysis (Truman et al., 1983). The control of ecdysis involves at least two peptide hormones. One is eclosion hormone (EH), which is secreted by just four brain neurosecretory cells, the VM cells (Truman and Copenhaver, 1989; Hewes and Truman, 1991). The VM cell axons project through the entire length of the CNS to form a peripheral neuroendocrine site associated with the hindgut. The second endocrine peptide is ecdysis triggering hormone (ETH) (Žitňan et al., 1996), which is secreted, together with other peptides (Žitňan et al., 1996; O'Brien and Taghert, 1998), by 18 Inka cells, located in epitracheal glands associated with the spiracles (Žitňan et al., 1996). These two endocrine sites mutually excite each other, resulting in one of the few known neuroendocrine positive-feedback systems (Ewer et al., 1997). EH release within the CNS may indirectly activate central portions of the ecdysis motor program by stimulating the release of a third peptide, crustacean cardioactive peptide (CCAP) (Gammie and Truman, 1999).

Our current evidence suggests that the control of EH release

by the declining ecdysteroid titer is indirect. During a brief period preceding EH release, the VM cells showed a transient and dramatic reduction in threshold and an activity-independent increase in action potential duration *in vivo* (Hewes and Truman, 1994). These two events required both the decline in circulating ecdysteroids and transcription, resulting from either direct action of steroid on the VM cells or indirect actions upon modulatory inputs upstream of EH release. The latter hypothesis was supported indirectly by a study that demonstrated undetectable levels of ecdysteroid receptor in the VM cells during the period of ecdysteroid sensitivity (Bidmon et al., 1991; Hewes and Truman, 1994).

The recent discovery of ETH has significantly advanced our understanding of these events. Ewer et al. (1997) showed that epitracheal gland extracts containing ETH could stimulate both a dramatic increase in VM cell excitability and activity-independent spike broadening *in vivo*. Similar results were obtained *in vitro* by bath application of synthetic ETH onto the brain (Ewer et al., 1997) and directly onto isolated VM cell somata (Gammie and Truman, 1999). These results show that ETH is sufficient to trigger changes in VM cell excitability that are comparable to the changes observed *in vivo* prior to the normal time of EH release. We do not know whether ETH is necessary for the increase in VM cell excitability and EH release, and the effects of ETH on the VM cells have not been tested in the presence of exogenous ecdysteroid or the absence of transcription. However, the most straightforward interpretation of the available evidence is that the decline in circulating ecdysteroids prior to ecdysis leads to EH release by stimulating the release of ETH, perhaps by direct action on the Inka cells or *via* signals from the epidermis to the epitracheal glands (Ewer et al., 1997).

The VM cells are an important model for understanding the integration of endocrine signals in a hierarchical neuroendocrine circuit. The release of EH is an explosive process in which more than 90 % of the available peptide stores are released over a period of just a few minutes (Truman and Copenhaver, 1989). The ionic currents that underlie VM cell activation and rapid EH secretion have not been explored. This report describes a method for acute isolation of the VM cell somata for whole-cell recording. In whole-cell current-clamp recordings, the acutely isolated VM cells displayed overshooting action potentials that were similar in shape and magnitude to action potentials observed in the VM cells *in vivo*. Thus, the membrane conductances present in the VM cell somata appear to have been preserved during the isolation procedure. Under voltage clamp, at least three voltage- and time-dependent conductances in the acutely isolated cells were observed. These were a voltage-dependent inward Ca^{2+} current (I_{Ca}), a Ca^{2+}-dependent outward K^+ current ($I_{K(Ca)}$) and a transient, voltage-dependent outward K^+ current (A current; I_A). This study is a comprehensive survey of the currents present in the VM cell somata and provides a basis for future voltage-clamp analyses of the cellular mechanisms underlying this unusual neuropeptide release process.

Materials and methods

Acute VM cell isolation

Larval tobacco hornworms, *Manduca sexta* (Johansson) (Lepidoptera: Sphingidae), were reared individually on an artificial diet (Bell and Joachim, 1976) at 26 °C with either a short-day (12 h:12 h light:dark) or a long-day (17 h:7 h light:dark) photoperiod. Larvae molting from the fourth to the fifth larval instar (pharate fifth instars) were staged relative to the time of ecdysis (0 h) according to morphological and behavioral markers (Copenhaver and Truman, 1982; Curtis et al., 1984). Animals were selected for recording within 10 min of the appearance of air in the old head capsule (–5.5 h; Copenhaver and Truman, 1982). At this time, the VM cells are competent to respond to ETH with a prolonged bout of tonic firing and EH release (Ewer et al., 1997; Gammie and Truman, 1999). However, tonic firing is not normally initiated until 30–60 min prior to ecdysis (Hewes and Truman, 1994).

The acute cell isolation procedure was performed as previously described (Hewes, 1993). Briefly, the brain was removed, arranged frontal surface up on a Sylgard-lined (Dow Corning, Midland, MI, USA) Petri dish, stabilized with minutien pins and immersed in normal recording solution (Table 1). The brain was manually desheathed, and the preparation was placed on a black background with oblique, fiber optic illumination. Under these conditions, the VM cell somata were visually identifiable at 40× under a dissecting microscope (Hewes and Truman, 1994). Using a fine minutien

Table 1. *Composition of solutions*

Bath solutions	Normal recording	Ca^{2+}-free recording	Na^+/Ca^{2+}-free recording	Na^+-free, Ba^{2+}-recording	Cd^{2+}-recording
NaCl	140	140	–	–	139.5
nMG^+	–	–	140	140	–
KCl	5	5	5	5	5
$CaCl_2$	4	–	–	–	4
$BaCl_2$	–	–	–	4	–
$CdCl_2$	–	–	–	–	0.5
$MgCl_2$	–	4	4	–	–
D-Glucose	28	28	28	28	28
Hepes	5	5	5	5	5

Intracellular solutions	K-pipette	Supplemented K-pipette	Supplemented Cs-pipette
KCl	140	140	–
CsCl	–	–	140
NaCl	5	5	5
$MgCl_2$	2	–	–
Hepes	20	20	20
EGTA	1	1	1
Mg-ATP	–	2	2
Cyclic AMP	–	0.1	0.1
Theophylline	–	2	2

nMG^+, N-methyl-D-glucamine.
Values are mmol l^{-1}.

pin, two small fragments of the neuronal cortex, each containing 1–3 VM cell somata (usually two; see Riddiford et al., 1994) and numerous adjacent neurons, were separated from the rest of the brain. To isolate the cells and to facilitate the formation of gigaohm pipette-membrane seals for patch-clamp recordings, these fragments were transferred to an 8 % papain solution (see below) in normal recording solution using a fire-polished, silane-treated (5 % in $CHCl_3$; to retard adhesion) micropipette with a tip diameter of approximately 100 μm. The 20–30 μm diameter VM cell somata, generally with less than 20 μm of the initial process still intact, were then isolated by gentle trituration. The remaining process usually retracted back into the soma within 5 min. The VM cells are much larger than any of the adjacent neurons (Hewes and Truman, 1994), and so they could be identified unambiguously throughout the trituration. After 5–6 min in the papain solution, the individual VM cells were transferred through three washes in normal recording solution before a final transfer to a 35 mm plastic Petri dish containing the same solution. The cells were allowed to settle and to adhere to the base of the dish in the center of a wedge-shaped region of clean (bare) plastic surrounded by a 2 mm deep layer of Sylgard. This arrangement facilitated the exchange of solutions during perfusion by reducing the volume of the chamber to 200 μl.

Perfusion was continuous during recordings and was gravity fed at the inlet and removed by vacuum aspiration at the outlet. The perfusion rate was 2–6 ml min^{-1}, and changes in the bath solution appeared to be complete within 1–3 min, judging by the lack of continued changes in ion currents in measurements repeated throughout the exchange.

Dissection and recording solutions

A crude 10 % papain (Calbiochem, San Diego, CA, USA) solution was subjected to dialysis with 12–14 kDa cut-off Spectrapor cellulose tubing (Spectrum Medical Industries, Los Angeles, CA, USA) in normal recording solution at 4 °C for 16 h. The osmolality of the papain solution after the completion of dialysis was 350 mosmol l^{-1} and, because the volume of the dializate was increased by 25 %, the final concentration of the papain solution was less than 8 %. Samples of the papain solution were stored at −20 °C for up to 3 weeks before showing any appreciable loss of effectiveness. Once thawed, however, the solution could only be kept on ice for 3–4 h.

The compositions of all internal and external recording solutions are given in Table 1. Modified Miyazaki saline (Miyazaki, 1980; Trimmer and Weeks, 1989) was used as the normal recording solution. Supplements to the K-pipette solution were included to retard the 'washout' of inward Ca^{2+} currents (see Results; Doroshenko et al., 1982; Byerly and Hagiwara, 1988). Supplemented K-pipette solution was used, except where indicated, for all experiments. The pH of each bath solution was adjusted to 7.4 with 1 mol l^{-1} NaOH, 1 mol l^{-1} HCl or 1.5 mol l^{-1} Tris base. The pH of each intracellular solution was adjusted to 7.2 with 1 mol l^{-1} KOH or CsOH, and samples of each intracellular solution were frozen at −20 °C until needed. The osmolalities of the seven different bath and intracellular solutions were tested using a Wescor 5500 vapor pressure osmometer (Logan, UT, USA) and averaged 350 mosmol l^{-1} and 300 mosmol l^{-1}, respectively. Hepes, EGTA, cyclic AMP, *N*-methyl-D-glucamine (nMG^+), adenosine 5′-triphosphate (Mg-ATP), 4-aminopyridine (4-AP) and theophylline were obtained from Sigma (St Louis, MO, USA).

Recording and analysis

The electrophysiological techniques used were essentially those described by Hamill et al. (1981) and Marty and Neher (1983). Patch pipettes were pulled from 50 μl micropipettes (VWR Scientific, Philadelphia, PN, USA) using a two-stage Narishige PP-83 microelectrode puller. The pipettes had resistances of 0.7–1.7 MΩ in the normal recording solution, and pipette–membrane seal resistances were usually greater than 2 GΩ.

Recordings were made using a Dagan 8900 patch-clamp/whole-cell clamp amplifier (Minneapolis, MN, USA) with the 8910 headstage (100 MΩ feedback resistor) at room temperature (23–25 °C) within an average of 38 min (range 26–58 min) of starting the dissection (see Hewes and Truman, 1994). Action potentials and voltage responses to injected current (in current-clamp mode) were stored on a VHS recorder after digitization on an Instrutech VR-10 digital data recorder (9600 baud; Instrutech Corporation, Mineola, NY, USA). Current was supplied using the bridge circuit in the Dagan amplifier. Data were analyzed off-line using SuperScope (100–1000 μs sample period; GW Instruments, Boston, MA, USA). Membrane currents recorded under voltage-clamp were stored and analyzed using pCLAMP 4.05 (Axon Instruments, Burlingame, CA, USA) software and a Tecmar (Labmaster, Solon, Cleveland, OH, USA) analog–digital/digital–analog converter. Current traces shown in the figures were filtered using an RC-filter supplied by the software (time constant 1.0 ms); however, all measurements were made on unfiltered data. All statistical data are reported as means ± S.E.M.

Command voltages were corrected for the junction potential between the intracellular and bath solutions just prior to seal formation using circuits within the Dagan amplifier. Capacitance current subtraction was done after gigaohm seal formation (but before breaking the cell membrane) using amplifier circuits. Leakage currents linear with the command voltage were subtracted arithmetically from currents used in calculations. Current wave forms shown in the figures were not leak-subtracted. Control experiments in Na^+/Ca^{2+}-free recording solution (N=1), Ca^{2+}-free recording solution (N=4) and normal recording solution following complete washout of I_{Ca} and $I_{K(Ca)}$ (N=6) showed that the leak current was linear from membrane voltages of −40 mV to +60 mV, and unsubtracted capacitance transients settled within 1.5 ms. The interpulse interval for the recording of inward and non-inactivating outward currents was 7.0 s, and the interprepulse interval for the measurement of transient outward currents was 3.0 s. In control experiments, these intervals were sufficient to

allow complete removal of current inactivation between pulses. A prepulse duration of 1.0 s was sufficient to completely remove transient outward current inactivation. The series resistance error (SRE) was estimated using the series resistance compensation circuit in the Dagan amplifier by assuming 70 % compensation (Byerly and Hagiwara, 1982). Trials in which the estimated SRE was greater than 4.0 MΩ were rejected. Cells were discarded when the space clamp was inadequate, as indicated by oscillations in the current wave forms.

Conductances (g) were determined using equilibrium potentials (E_K, E_{Ba}) calculated with the Nernst equation (Hille, 1992). The intracellular K^+ concentration was assumed to be equal to the K^+ concentration in the pipette solution. The intracellular Ba^{2+} concentration was assumed to be 10 pmol l^{-1}. The conductance/voltage (g/V) curve shown in Fig. 6F was fitted to a first-order Boltzmann equation of the following form:

$$\frac{g}{g_{max}} = [1 + \exp(-n(V - V_{50})/kT)]^{-1} , \quad (1)$$

where g_{max} is the maximal conductance, V_{50} is the voltage of half-maximal inactivation of the peak current, n is a slope factor, T is the absolute temperature, and k is the Boltzmann constant.

Membrane capacitance (C) was calculated using the amplitude of the square-wave current (dI) obtained from a triangle-wave voltage command in patch-clamp recordings as follows (Moody and Bosma, 1985):

$$dI = 2C \frac{dV}{dt} . \quad (2)$$

The membrane surface area was then calculated using the membrane capacitance, assuming that the specific capacitance of the membrane was 1.0 μF cm^{-2} (Almers, 1978).

Whole-cell current-clamp recordings were performed immediately after obtaining complete electrical access to the interior of the cell, for a maximum of 40 s, and prior to patch-clamp recording. The cells were stimulated with 600–1000 ms hyperpolarizing and depolarizing current steps of varying magnitudes with an interpulse interval of approximately 3 s. Threshold voltage and spike duration were measured as described previously (Hewes and Truman, 1994). Cells that failed to fire overshooting action potentials (spontaneous or elicited) at this time were discarded.

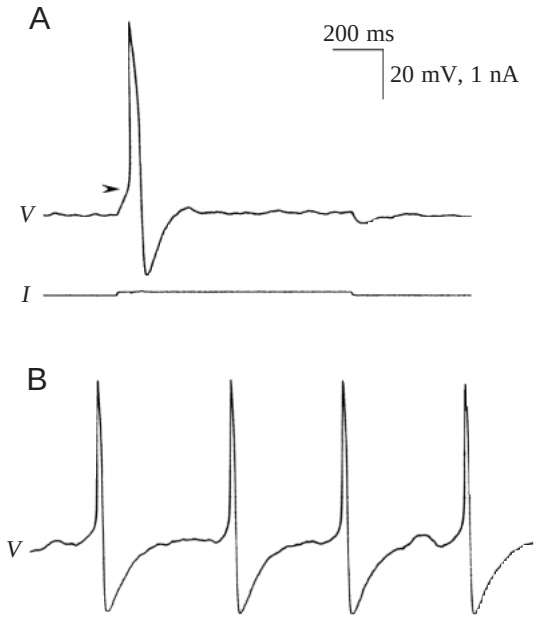

Fig. 1. Whole-cell current-clamp recordings from the acutely isolated VM cell somata. (A) Action potential elicited by current injection into a cell that was not tonically active at rest. Note that the membrane potential reached a plateau that was several millivolts negative of the membrane potential at threshold (arrowhead). (B) Spontaneous, tonic firing of action potentials in a spontaneously active cell. The recordings were performed in normal recording solution (see Table 1). V, membrane voltage; I, injected current.

Results

Current-clamp recordings

Whole-cell current-clamp recordings from acutely isolated VM cell somata from pharate fifth-instar larvae are shown in Fig. 1. Many cells were refractory to electrical stimulation and fired only one (or infrequently two) action potentials during sustained depolarizations (Fig. 1A). In these recordings, after the action potential, the membrane voltage reached a plateau value that was hyperpolarized relative to that preceding the spike (arrowhead, Fig. 1A). A similar phenomenon was also observed in intracellular recordings from the VM cell somata in the isolated brain (Hewes and Truman, 1994). In other recordings, the acutely isolated cells fired tonically at rest at 1.7±0.3 Hz (N=7), a rate within the range of the firing rates observed in intracellular recordings from spontaneously active cells *in situ* (Hewes and Truman, 1994; Ewer et al., 1997; Gammie and Truman, 1999). The mean spike amplitude was 96.9±2.8 mV (N=13), the mean duration of the action potential was 31.3±2.5 ms and the mean threshold was 7.5±2.4 mV (median=8.3 mV) depolarized with respect to the resting membrane potential. These values were also within the ranges reported previously for these neurons. The overall similarities between the electrical characteristics of the cells recorded with these two methods indicate that the voltage-dependent currents present in the acutely isolated VM cell somata were representative of the currents present in the VM cell somata *in vivo*.

In addition to the general similarities between the electrical characteristics observed in acutely isolated somata and those observed in recordings from the cells *in situ*, there were also differences between them. The mean input resistance of the acutely isolated cells (131±22 mΩ; N=7) was approximately twofold greater than the mean input resistance observed in the intracellular recordings (Hewes and Truman, 1994). This may have been caused by differences in leakage currents that were associated with formation of a gigaohm seal *versus* intracellular penetration or due to the removal of the cell

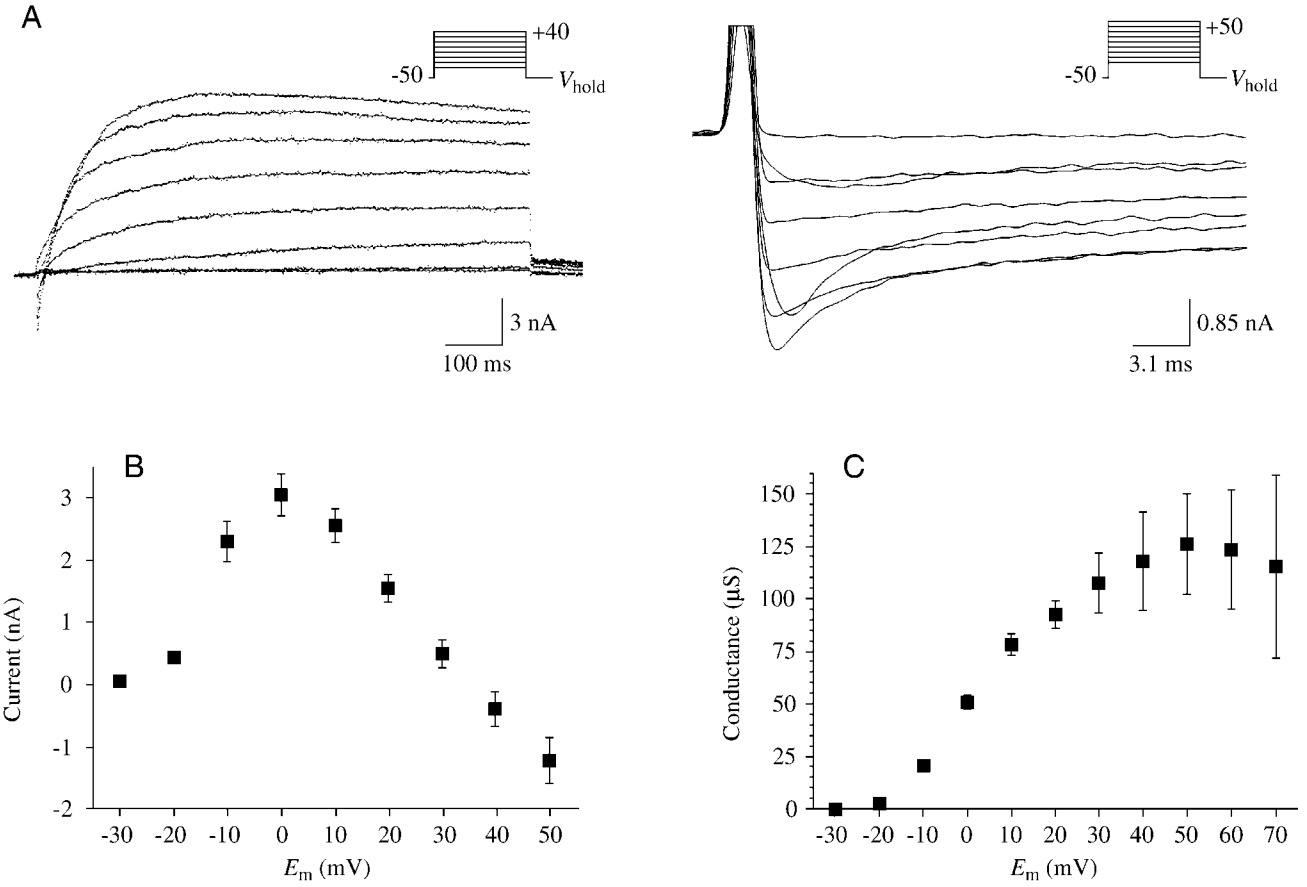

Fig. 2. Whole-cell membrane currents of the VM cell somata. (A) Whole-cell currents elicited in normal recording solution (Table 1) with supplemented K-pipette solution (left) or supplemented Cs-pipette solution (right; equimolar substitution of Cs^+ for K^+). Insets, voltage pulse protocols (V_{hold} and maximum voltage indicated; 10 mV incremental steps). (B) Current/voltage (*I*/*V*) relationship for the peak inward current. (C) Conductance/voltage relationship for the steady-state outward current. Conductances were calculated assuming that the reversal potential was at E_K=−84 mV (see Materials and methods). Values in B and C are the means ± S.E.M. from 11 experiments. E_m, membrane potential.

arborization. At the resting membrane potential, 54 % of the acutely isolated somata (*N*=13) fired tonic action potentials. In contrast, tonic firing was never observed in recordings from the VM cells *in situ* at the same developmental stage (Hewes and Truman, 1994). These changes in excitability may have been due to changes in the driving force for some ionic currents following perfusion of the interior of the cell by the whole-cell pipette or they may have been due to factors associated with isolation of the soma from the rest of the cell (see Discussion). However, under voltage-clamp, all the cells displayed the same set of voltage-dependent conductances (see below), and there was no clear correlation between the properties of these conductances and the firing behavior of the same cells under current-clamp (data not shown).

Voltage-clamp recordings

When depolarizing voltage steps were delivered from a holding potential of −50 mV, a fast transient inward current was observed, followed by a sustained outward current (Fig. 2A). The transient inward current was first activated during voltage steps to −20 mV, and the maximum current was observed during voltage steps to 0 mV (Fig. 2B). At −20 mV, the latency-to-peak inward current was 6.5 ms; at more depolarized voltages, the latency reached a minimum of 3.0 ms. The sustained outward current was also first activated during voltage steps to −20 mV, the maximum conductance was observed at +50 mV, and the conductance/voltage relationship at voltage steps greater than +50 mV displayed a negative slope (Fig. 2C). The average inactivation of the outward current in sustained, 800 ms pulses was less than 30 % (Fig. 2A). Using ion substitution and appropriate voltage protocols, three voltage-dependent components were isolated from the inward and outward currents.

Inward current (I_{Ca})

Both the inward current and most of the outward current were reversibly blocked in Na^+/Ca^+-free recording solution (Fig. 3A; *N*=2), Ca^+-free recording solution (Fig. 3B; *N*=3) and Cd^{2+} recording solution (0.5 mmol l^{-1} Cd^{2+}; Fig. 3C; *N*=7), although a small, transient outward current persisted in Cd^{2+} recording solution (I_A; see below). These results suggest that the inward currents were carried solely through voltage-dependent Ca^{2+} channels (I_{Ca}). In some recordings, small inward and outward currents (Fig. 3A,B, center traces)

persisted in the nominally Ca^{2+}-free recording solutions. It is likely that these currents were due to residual Ca^{2+} in the bath, since no Ca^{2+}-chelating agent was used in the bath solutions. However, the possible contributions of small inward Na^+ currents and sustained outward K^+ currents cannot be excluded. When Ba^{2+} was substituted for Ca^{2+} (Na^+-free, Ba^{2+}-recording solution), the resulting Ba^{2+} current (I_{Ba}) was inward and displayed slow, moderate inactivation over the duration of 800 ms depolarizations (Fig. 5; *N*=18). During the transition from the normal recording solution to the Na^+-free, Ba^{2+} recording solution, the inward current was large and appeared to inactivate (data not shown). A few seconds later, the inward current settled to the smaller, slowly inactivating current. The larger current during the transition was therefore likely to be residual I_{Ca}.

When $I_{K(Ca)}$ was blocked with supplemented Cs-pipette solution (see below), I_{Ca} showed complete inactivation during 800 ms voltage pulses (Fig. 4A), and no steady-state current was observed (data not shown). From a holding potential of –50 mV, I_{Ca} was first activated during voltage steps to –20 mV,

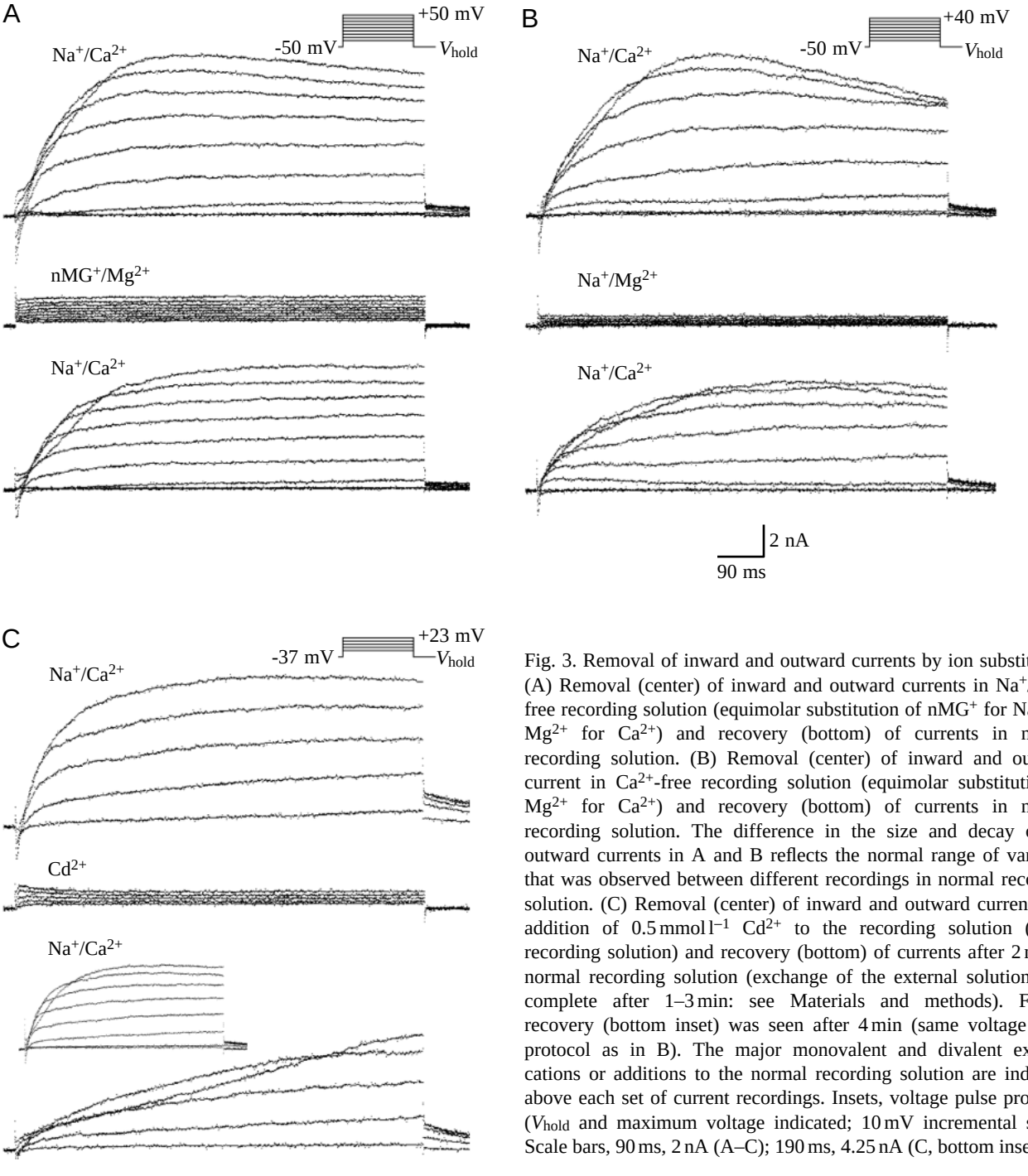

Fig. 3. Removal of inward and outward currents by ion substitution. (A) Removal (center) of inward and outward currents in Na^+/Ca^{2+}-free recording solution (equimolar substitution of nMG^+ for Na^+ and Mg^{2+} for Ca^{2+}) and recovery (bottom) of currents in normal recording solution. (B) Removal (center) of inward and outward current in Ca^{2+}-free recording solution (equimolar substitution of Mg^{2+} for Ca^{2+}) and recovery (bottom) of currents in normal recording solution. The difference in the size and decay of the outward currents in A and B reflects the normal range of variation that was observed between different recordings in normal recording solution. (C) Removal (center) of inward and outward current after addition of 0.5 mmol l^{-1} Cd^{2+} to the recording solution (Cd^{2+}-recording solution) and recovery (bottom) of currents after 2 min in normal recording solution (exchange of the external solutions was complete after 1–3 min: see Materials and methods). Further recovery (bottom inset) was seen after 4 min (same voltage pulse protocol as in B). The major monovalent and divalent external cations or additions to the normal recording solution are indicated above each set of current recordings. Insets, voltage pulse protocols (V_{hold} and maximum voltage indicated; 10 mV incremental steps). Scale bars, 90 ms, 2 nA (A–C); 190 ms, 4.25 nA (C, bottom inset).

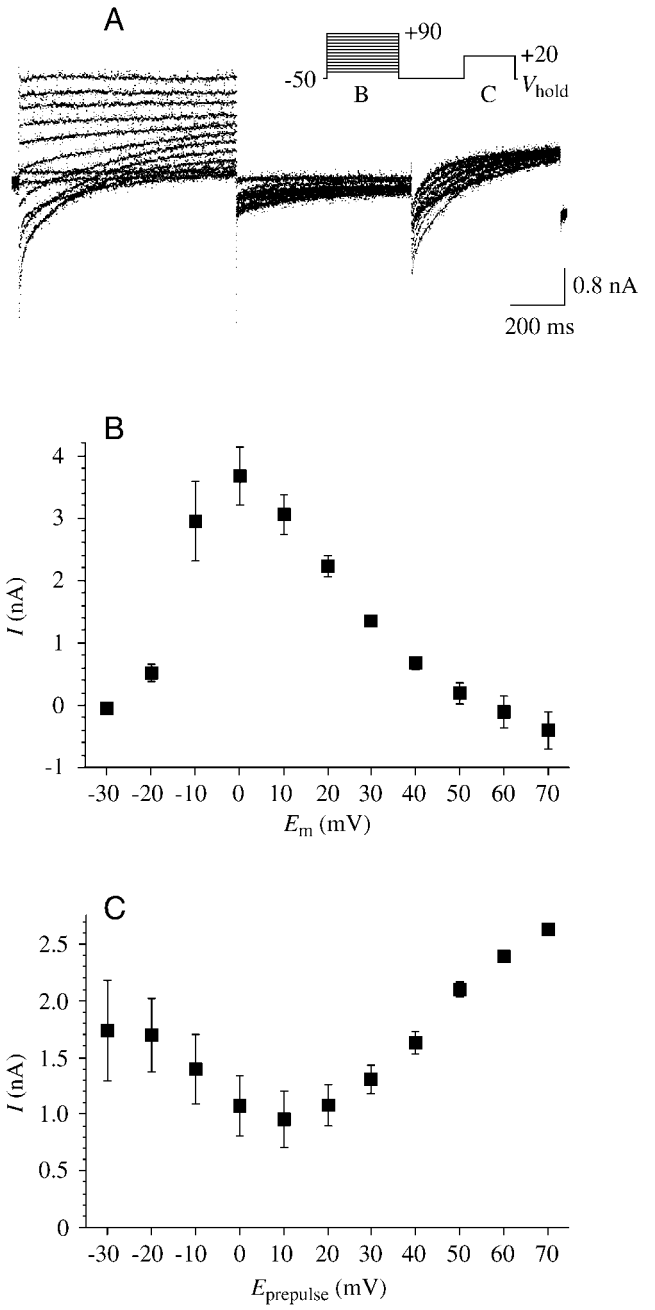

Fig. 4. Voltage-dependent activation and Ca^{2+}-dependent inactivation of I_{Ca}. (A) Current traces for I_{Ca} after removal of $I_{K(Ca)}$ with supplemented Cs-pipette solution (equimolar substitution of Cs^+ for K^+) in normal recording solution. (B) Current/voltage relationship (*I*/*V*) for peak I_{Ca} during the voltage prepulses (*N*=3). (C) Current/voltage relationship for Ca^{2+}-dependent inactivation of I_{Ca} at +20 mV. Values are means ± S.E.M. (*N*=3). Inset in A, voltage prepulse/pulse protocol with points of measurement for B and C indicated (V_{hold} and maximum voltages indicated; 10 mV incremental steps); E_m, membrane potential; $E_{prepulse}$, prepulse membrane voltage.

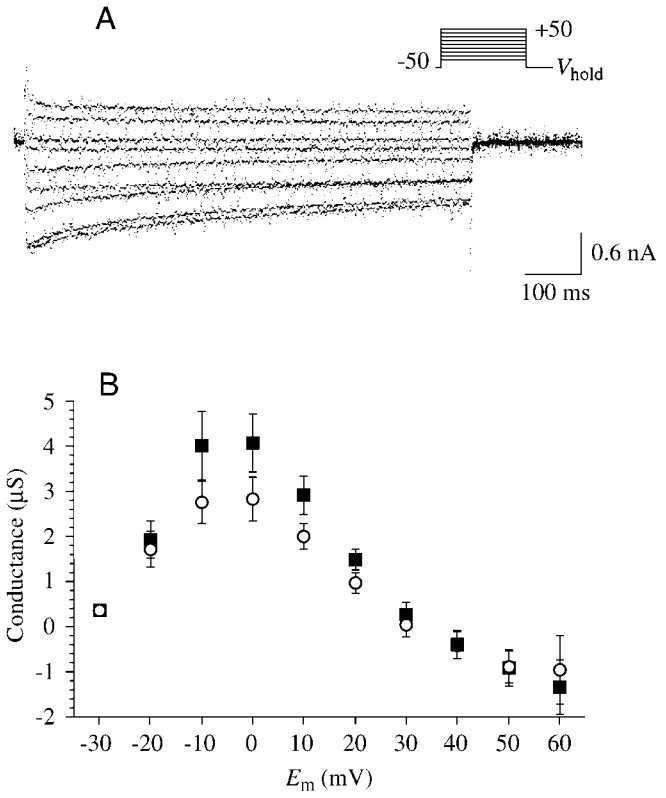

Fig. 5. Voltage-dependent activation of inward Ba^{2+} currents. (A) Current traces for I_{Ba} recorded in Na^+-free, Ba^{2+}-recording solution. (B) Conductance/voltage (*g*/*V*) relationships for I_{Ba} at peak current (filled squares) and at steady state (open circles; measured at 780 ms). Values in B are means ± S.E.M. from five experiments. Inset in A, voltage pulse protocol (V_{hold} and maximum voltage indicated; 10 mV incremental steps).

the peak current was obtained during voltage steps to 0 mV, and the potential for 50 % activation of the current was −13 mV (Fig. 4B). The rapid inactivation of the current appeared to be at least partially Ca^{2+}-dependent, because I_{Ba} displayed less than 35 % inactivation (Fig. 5A). When the peak inward Ca^{2+} current (at +20 mV; V_{hold}=−50 mV) was plotted as a function of prepulse voltage, the resulting activation curve showed a pronounced 'V-shape', with a minimum at +10 mV (Fig. 4C). This phenomenon is typical of currents displaying Ca^{2+}-dependent inactivation, and it is due to the reduced influx of Ca^{2+} as the prepulse voltage approaches E_{Ca} (Eckert and Chad, 1984).

To characterize the inward current in the absence of outward currents and Ca^{2+}-dependent inactivation more fully, Ba^{2+} was substituted for Ca^{2+} as the charge carrier. The ionic substitution was performed at least 2 min before rupturing the cell membrane for whole-cell recording to allow sufficient time for the replacement of external Ca^{2+} with Ba^{2+}. The peak inward conductance carried by Ba^{2+} was 6.5-fold smaller than the inward Ca^{2+} conductance (data not shown). However, the activation curves showed a similar voltage dependence. From a holding potential of −50 mV, I_{Ba} was first activated during voltage steps to −20 mV, the peak conductance was obtained during voltage steps to −10 to 0 mV, and the potential for 50 % activation of the conductance was −18 mV (Fig. 5B). In

contrast to I_{Ca} (Fig. 4A), I_{Ba} displayed only moderate inactivation during 800 ms depolarizing voltage steps; at 0 mV, the steady-state Ba^{2+} conductance was 30 % lower than the peak conductance (Fig. 5A). The conductance/voltage relationship for I_{Ba} displayed a steep negative slope at membrane potentials above 0 mV. This result indicates that I_{Ba} displays voltage-dependent inactivation since (i) the equilibrium potential for Ba^{2+} should have been considerably more positive than 0 mV (see Materials and methods), and (ii) the replacement of Ca^{2+} with Ba^{2+} may have prevented Ca^{2+}-dependent inactivation of the conductance (Eckert and Chad, 1984; Mills and Pitman, 1997).

Sustained outward current ($I_{K(Ca)}$)

The sustained outward current was eliminated in solutions that either removed or blocked I_{Ca} (Fig. 3A–C). In other systems, the conductance of Ba^{2+} through Ca^{2+} channels is large, yet the influx of Ba^{2+} does not activate Ca^{2+}-dependent channels (Hagiwara and Byerly, 1981; Hagiwara and Ohmori, 1982; Latorre et al., 1989; Hayashi and Levine, 1992). Here, inward Ba^{2+} currents were observed in Na^+-free, Ba^{2+} recording solution, but the sustained outward current was removed (Fig. 5). This result indicates that the sustained outward current was Ca^{2+}-dependent. In other cells, the conductance/voltage relationships for Ca^{2+}-dependent outward currents display a negative slope at highly depolarized voltages. This is due to a reduction in the driving force for Ca^{2+} entry at membrane potentials approaching E_{Ca} (Thomas, 1984). The whole-cell patch-clamp recordings from the VM cell somata often became unstable at these voltages, so the shape of the *I/V* relationship above 70 mV was not determined. In recordings that remained stable above 70 mV, the decline in the amplitude of the steady-state current was pronounced (data not shown).

When the electrode was filled with supplemented Cs-pipette (0 mmol l^{-1} K^+) solution, most or all of the outward current was blocked (Fig. 4A; N=6). This result suggests that the Ca^{2+}-dependent outward current was carried by K^+ ($I_{K(Ca)}$). In normal recording solution with K-pipette solution, the reversal potential for the steady-state outward current (measured as the instantaneous tail current following prepulses to +20 mV) was −65 mV (data not shown). This is 19 mV positive of the calculated equilibrium potential (E_K) and may reflect the contribution of other permeant cations. Alternatively, since the VM cell somata display substantial membrane infolding (see below), the depolarized reversal potential may have been caused by elevation of the external K^+ concentration in infoldings of the surface membrane (Thomas, 1984).

Transient outward current (I_A)

A transient outward current was activated following large hyperpolarizing prepulses (to remove the current from inactivation) from holding potentials of −40 to 0 mV (Fig. 6A). In normal recording solution, the reversal potential for the transient outward current was −64 mV (Fig. 6G), a value 18 mV positive of E_K (see above). The latency from the offset of the hyperpolarizing prepulse to the peak current was approximately 8 ms, and the latency was not dependent upon the prepulse voltage. When the electrode was filled with supplemented Cs-pipette solution, this current was blocked (Fig. 6B; N=4). These properties suggest that the transient outward current belongs to a well-characterized family of K^+ currents, the A currents (I_A; see Connor and Stevens, 1971a,b; Adams et al., 1980). In many invertebrate neurons, 4-AP blocks A currents in a voltage- and time-dependent manner (Thompson, 1982). Addition of 5 mmol l^{-1} 4-AP to the normal recording solution blocked some of the transient outward current, and a new, more slowly inactivating component appeared (Fig. 6C; N=4). In other cells, a similar change in the time course of I_A inactivation appears to be caused by voltage-dependent blocking effects of 4-AP (Thompson, 1982). Removal of I_{Ca} and $I_{K(Ca)}$ with Na^+/Ca^{2+}-free recording solution (N=2) and Cd^{2+} recording solution (N=6) failed to block I_A at a V_{hold} of −20 mV (Fig. 6D,E). However, the potential for the half-removal of inactivation in Na^+/Ca^{2+}-free recording solution was shifted by −25 mV from the control level (cf. Fig. 6A) to −88 mV. Similar shifts have been observed in other cells and appear to be due to differences in the neutralization of negative membrane surface charges following the exchange of divalent cations, such as Ba^{2+}, for Ca^{2+} (Ohmori and Yoshii, 1977; but see Simoncini and Moody, 1991).

It was possible to measure I_A in relative isolation from a holding potential of −20 mV. The contaminant inward tail current appeared to be maximally activated at −50 mV, since the tail currents with −40 mV and −50 mV prepulses were equal (−0.69±0.08 with −40 mV and −0.67± 0.04 with −50 mV; N=6; Fig. 6A, arrowhead). The value for the peak inward current at −50 mV was therefore subtracted from each of the peak A-current values in Fig. 6F. The voltage-dependence of the steady-state inactivation was well fitted by a first-order Boltzmann equation (equation 1). Removal of I_A inactivation at both stages was first observed with −60 mV prepulses. Removal of inactivation was 50 % complete at −63 mV, and peak current was 3.8 nA. Removal of inactivation was nearly complete with hyperpolarization to −80 mV (Fig. 6F). The resting potential of the VM cells *in situ* was −37 mV (Hewes and Truman, 1994), and the peak after-spike hyperpolarization in the acutely isolated cells (measured at rest) was 30.1±1.7 mV negative of rest (approximately −67 mV, N=5). The minimum prepulse duration necessary for more than 95 % removal of I_A inactivation (V_{hold}=−20 mV, prepulse −90 mV) was 100–150 ms, and prepulses of 10 ms were sufficient to remove some inactivation (data not shown).

Membrane surface area

The membrane capacitance measured in the whole-cell voltage-clamp recordings was $1.16\times10^{-4}\pm0.24\times10^{-4}$ cm^2 (N=9). The mean diameter of the acutely isolated VM cell somata was 30.4±1.3 μm (N=5). Assuming that the cells were perfect spheres, the predicted surface area was 0.28×10^{-4} cm^2. This value is approximately 75 % smaller than the area

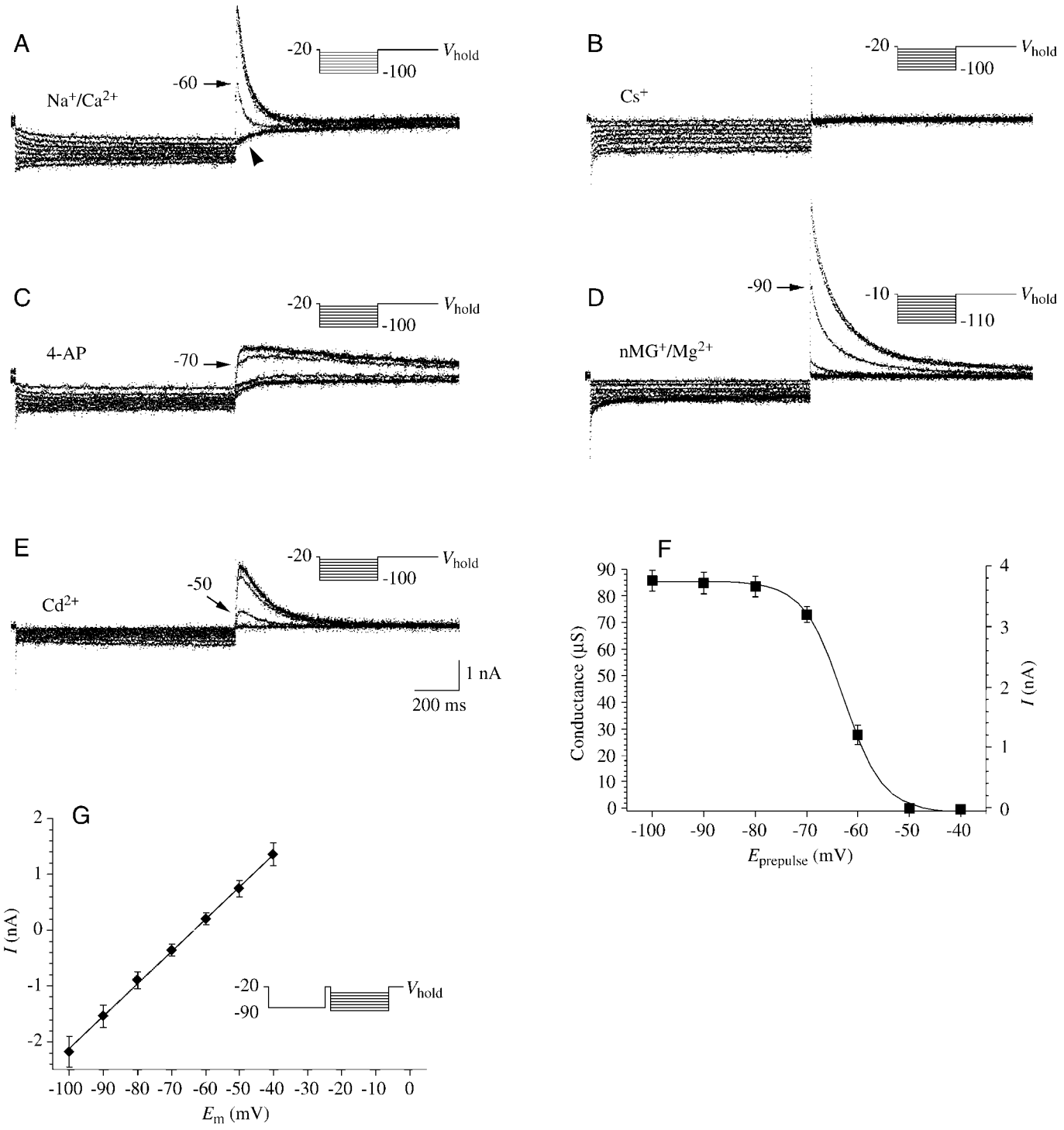

Fig. 6. Transient K^+ current (I_A). (A) Current traces for I_A in normal recording solution. (B) Removal of I_A with supplemented Cs-pipette solution (equimolar substitution of Cs^+ for K^+). (C) Partial removal of I_A and changes in current kinetics in 5 mmol l^{-1} 4-aminopyridine (4-AP). (D) Presence of I_A in Na^+/Ca^+-free recording solution (equimolar substitution of nMG^+ for Na^+ and Mg^{2+} for Ca^{2+}). (E) Presence of I_A in 0.5 mmol l^{-1} Cd^{2+} (Cd^{2+}-recording solution). (F) Conductance/voltage relationship (g/V) for steady-state inactivation of I_A in normal recording solution (N=6). The curve is a fit of a first-order Boltzmann equation with the following variables: V_{50}=−62.9 mV; N=6.3; g_{max}=84.8 μS. The voltage prepulse/pulse protocol is shown in A. Inward currents measured at −50 mV (arrowhead in A) were subtracted from the peak I_A values (see Results). (G) Current/voltage relationship for the instantaneous I_A tail currents following a 1 s, −90 mV prepulse and a 25 ms return to V_{hold} (−20 mV) in normal recording solution (N=7). The major external cations, internal cations or additions to the normal recording solution are indicated above each set of traces (A–E). Insets, voltage prepulse/pulse protocols (V_{hold} and maximum prepulse voltage indicated; 10 mV incremental steps).

calculated from the capacitance measurements and indicates a considerable amount of membrane infolding.

Discussion

This report describes a method for the rapid isolation of the eclosion hormone neuron (VM cell) somata for whole-cell patch recording. The VM cells were identified unequivocally on the basis of their large size and location within the brain (Hewes and Truman, 1994), and the cells were followed visually throughout the isolation procedure. In whole-cell current-clamp recordings performed immediately after the isolation of the VM cells, the electrophysiological properties of the cells were similar to the properties observed in recordings from the VM cells *in situ*. In whole-cell voltage-clamp recordings, three voltage-dependent currents were isolated and characterized using voltage and ion-substitution protocols. The results presented here provide the basis for future investigations into the cellular mechanisms underlying EH release and the integration of this release within the complex hierarchy of neuropeptide/peptide hormone actions controlling ecdysis.

Threshold and firing properties of the acutely isolated VM cell somata

The electrical properties of the VM cell somata have been described previously using intracellular recording techniques (Hewes and Truman, 1994; Ewer et al., 1997; Gammie and Truman, 1999). Following acute isolation of the VM cell somata and rupturing of the cell membrane for whole-cell recording, the electrical properties of the VM cells were well preserved (Fig. 1). Like the cells recorded intracellularly *in situ*, the acutely isolated cells displayed long-duration, overshooting action potentials with large afterhyperpolarizations. These characteristics are typical of insect neurosecretory cells, but are rarely found in other insect neurons (e.g. Miyazaki, 1980). In addition, many of the acutely isolated somata fired only single action potentials during prolonged membrane depolarizations. Subsequent to the afterhyperpolarization, the membrane potential reached a plateau value that was hyperpolarized relative to the threshold value. This property was characteristic of the recordings from the VM cells *in situ* (Hewes and Truman, 1994). These findings indicate that the ionic currents present in the acutely isolated VM cell somata were a good representation of the ionic currents present in these neurons *in vivo*.

In addition to the above similarities, there were changes in the electrical characteristics of the VM cell somata that were associated with the physical isolation procedure, the intracellular perfusion of the cytoplasm by the contents of the whole-cell pipette, or both. Unlike the cells at the same developmental stage *in situ* (5.5 h prior to ecdysis; Hewes and Truman, 1994), 54 % of the acutely isolated cells fired action potentials tonically at rest (albeit at rates comparable to those observed *in situ* 5 h later, during pre-ecdysis). In addition, both the threshold voltage and the duration of the action potential were similar to the values recorded *in situ* after the onset of pre-ecdysis (Hewes and Truman, 1994), during or immediately prior to the normal time of EH release (see Ewer et al., 1997).

These differences in electrical characteristics may reflect alterations in the internal ionic composition (caused by perfusion of the cell interior by the contents of the whole-cell pipette), which could change the driving forces for membrane currents or remove components of intracellular signaling pathways. The intrinsic electrical properties of the VM cells may also have been physically altered by the acute isolation procedure. This could have occurred following the elimination of tonic synaptic and paracrine inputs to the VM cells or removal of most of the VM cell axon and its contribution to the electrical properties measured in the soma. Finally, the exposure of the VM cells to papain may have altered ion currents. The papain treatment was comparable to treatments commonly employed in other systems (see Sachs and Auerbach, 1983), and in most cases channel proteins function remarkably well following the exposure of their extracellular domains to proteolytic enzymes (but see Allen et al., 1988). Each of the above possible alterations could affect the behavior of the cells under current-clamp without altering the voltage dependence or kinetics of the currents normally present in the soma. However, because the percentage of acutely isolated cells (at −5.5 h) that fired spontaneously was comparable with the percentage obtained in the intracellular recordings during pre-ecdysis, the acute isolation technique could not be used to determine the ionic currents directly responsible for the endogenous changes in spike threshold.

Future experiments using ETH to activate EH secretion from the VM cells may overcome this technical limitation. Our current evidence indicates that ETH, perhaps in association with additional peptide hormones, directly triggers EH release *in vivo* (Gammie and Truman, 1999). This model is supported by the fact that ETH caused changes in the electrical characteristics of the VM cells that were qualitatively similar to the endogenous changes in VM cell excitability observed *in situ* prior to ecdysis. When VM cells were isolated from animals shortly after the onset of pre-ecdysis, they displayed a 40 % increase in the duration of the action potential and activity-independent spike broadening, and 50 % of the neurons fired tonically at rest (Hewes and Truman, 1994). It appears likely that these endogenous changes in the electrical characteristics of the VM cells were recorded largely before the onset of EH release and during a period of gradually increasing excitability. During the responses to epitracheal gland extracts and synthetic ETH, the VM cells displayed a progressive broadening of the soma spike before the onset of spontaneous, tonic firing (Ewer et al., 1997; Gammie and Truman, 1999). This gradual change in excitability is also likely to occur *in vivo* during an approximately 15–20 min interval between the onset of pre-ecdysis and the onset of detectable EH release (Ewer et al., 1997). Taken together, these findings indicate that ETH causes changes in VM cell excitability that (i) are comparable to the changes observed *in vivo*, and (ii) are considerably more pronounced than the

changes in excitability associated with acute isolation of the VM cell somata or whole-cell recording.

Overview of VM cell membrane currents

The VM cells contained only three major time- and voltage-dependent conductance types. These were I_{Ca}, $I_{K(Ca)}$ and I_A. Interestingly, there was no clear indication of either an inward Na^+ current (I_{Na}) or a delayed rectifier K^+ current (I_K). This is unusual for a peptidergic neuron, since in many neurosecretory cells the inward current is carried by a mixture of I_{Na} and I_{Ca}, and the outward current usually includes some I_K (Trifaró and Poisner, 1985). In normal recording solution, I_{leak} was linear from −40 mV to +60 mV. Since there were no changes in R_{input} correlated with the changes in VM cell excitability in the isolated brain (Hewes and Truman, 1994), this current was not investigated further.

Analysis of I_A

The VM cell somata contained a substantial transient outward current that resembled the well-characterized A current of insects and many other eukaryotic organisms (Hille, 1992). A common feature of I_A is its inactivation at subthreshold membrane voltages (Connor and Stevens, 1971a). In the VM cell somata, I_A was completely inactivated at a holding potential of −20 mV. No recovery from inactivation was observed following 1.0 s prepulses to −50 mV, a value more than 10 mV negative to the normal resting potential of these cells. Recovery from inactivation was first observed with −60 mV prepulses, and prepulses to −63 mV removed 50 % of I_A inactivation. These properties are similar to the 'A_2' form of I_A observed in many insect neurons and preneuronal cells (Solc and Aldrich, 1988; Tsunoda and Salkoff, 1995). Hyperpolarizing prepulses as short as 10 ms partially removed I_A from inactivation, and in current-clamp recordings the VM cell after-spike hyperpolarization briefly carried the membrane to voltages around −65 mV. These data suggest that I_A is activated following the generation of an action potential. Consequently, this current may influence the repetitive firing frequency in tonically active cells during the period of EH release (Connor and Stevens, 1971b).

Analysis of $I_{K(Ca)}$

Given the absence of a delayed rectifier K^+ current, $I_{K(Ca)}$ was the only sustained K^+ current present in the VM cell somata. When Cs^+ was substituted for K^+ in the pipette, $I_{K(Ca)}$ was blocked completely, leaving only I_{Ca}. In addition, I_{Ca} was completely inactivated during 800 ms voltage steps (Fig. 4A). Thus, the steady-state whole-cell outward current (e.g. Fig. 2A; minus the leakage current) was solely $I_{K(Ca)}$. When measured as the steady-state whole-cell outward current (at 780 ms), $I_{K(Ca)}$ was first activated at −20 mV and was maximally activated at 0 mV (Fig. 2B). The $I_{K(Ca)}$ was similar in size and voltage-dependence to the slow Ca^{2+}-mediated conductance observed in other insect cells (Thomas, 1984; Nightingale and Pitman, 1989; Singh and Wu, 1989), and displayed the expected bell-shaped activation curve (Fig. 2C) that is caused by the reduced entry of Ca^{2+} into cells during larger depolarizations (Heyer and Lux, 1976). Once activated by voltage and Ca^{2+} entry, $I_{K(Ca)}$ displayed only moderate decay during sustained depolarizations above the normal resting potential. In contrast, I_A was rapidly inactivated. Thus, $I_{K(Ca)}$ appears to be responsible for the membrane hyperpolarization (relative to threshold) that is sustained in some cells for several seconds (Hewes and Truman, 1994) during prolonged depolarizations from the resting membrane potential (Fig. 1A). In intracellular recordings from the isolated brain prior to the onset of EH release (−5.5 h), some cells fired multiple action potentials during large sustained depolarizations, and the amplitude of the additional action potentials was often considerably smaller than the amplitude of the first action potential (Hewes and Truman, 1994). It is likely that $I_{K(Ca)}$ causes this phenomenon by shunting current flow across the soma membrane (after the first action potential) and thereby reducing the amplitude of secondary spikes propagating into the soma from the initial process or axon.

Analysis of I_{Ca}

When supplemented Cs-pipette solution was used to block all voltage-dependent outward currents, there appeared to be almost complete inactivation of I_{Ca} in 1 s pulses (Fig. 4A). The inactivation of I_{Ba} was much less pronounced (Fig. 5A), which is consistent with the considerable Ca^{2+}-dependence of the inactivation (I_{Ca}) seen in normal recording solution (Fig. 4C). Both I_{Ca} and I_{Ba} were first activated during voltage steps to −20 mV, and the peak currents were measured during voltage steps to 0 mV. The reversal potential for I_{Ca} was +53 mV (Fig. 4) and the reversal potential for I_{Ba} was +30 mV (Fig. 5). Equally low equilibrium potentials have been measured for other insect calcium currents (cf. Byerly and Leung, 1988) and may be due either to imperfect ionic selectivity or to local accumulation of Ca^{2+} near the cytoplasmic surface. In general the characteristics of I_{Ba} and I_{Ca} match those described in other insect neuron somata (Byerly and Leung, 1988; Christensen et al., 1988; Leung et al., 1989; Hayashi and Levine, 1992). The unitary conductance of Ba^{2+} through Ca^{2+} channels is usually equal to or greater than the conductance of Ca^{2+} (Hess et al., 1986; Fox et al., 1987a,b). Thus, I_{Ba} is often larger than I_{Ca} (see Kloppenburg and Hörner, 1998). However, as is the case in some cells (e.g. Richard et al., 1990), this sequence was reversed for the VM cell somata. This may be due to differences in ion selectivity among calcium channels or due to differential effects of Ca^{2+} on surface charge or on channel-gating characteristics.

Determination of threshold and action potential duration

The location of the VM cell spike initiation zone(s) is not known. However, in intracellular recordings from isolated VM cell somata, Gammie and Truman (1999) showed that ETH triggers changes in excitability that were comparable to those observed in intracellular recordings from the isolated brain. Thus, the VM cell somata possess all the currents necessary to generate spontaneous tonic firing, and the currents present in

the soma are likely to be representative of the currents found at the spike initiation zone(s).

Three sets of observations indicate that I_{Ca} and/or $I_{K(Ca)}$ mediate the decrease in spike threshold and the increase in the duration of the action potential at the normal time of EH release. First, the currents must be voltage dependent, since the leakage current (measured as the input resistance) does not change during this period (Hewes and Truman, 1994). Second, the changes in the electrical properties of the VM cell somata appear to be due to changes in existing currents. In pilot experiments performed on somata that were isolated after the onset of pre-ecdysis, no additional voltage-dependent currents were observed (Hewes, 1993; R. S. Hewes, unpublished observations). Finally, I_A does not appear to regulate spike threshold or the duration of the action potential. At rest I_A is fully inactivated; in quiescent cells (–5.5 h), the voltage of removal of I_A from inactivation (Fig. 6F) is more than 10 mV hyperpolarized relative to the resting potential (–37 mV). Therefore, I_A is not activated in quiescent cells (see Grolleau and Lapied, 1995) and it cannot be further inactivated to mediate activity-dependent spike broadening during tonic firing (Ma and Koester, 1996).

I thank Drs James W. Truman and William J. Moody for their support, helpful discussions and comments on the manuscript. I also thank Drs A. O. Dennis Willows, Aguan Wei and Jeanne Nerbonne for their comments. These experiments were conducted in the laboratory of J. W. Truman, with support from NSF grant IBN92-19742 to J.W.T. and NIH training grant T32 GM 07108.

References

Adams, D. J., Smith, S. J. and Thompson, S. H. (1980). Ionic currents in molluscan soma. *Annu. Rev. Neurosci.* **3**, 141–167.

Allen, C. N., Brady, R., Swann, J., Hori, N. and Carpenter, D. O. (1988). *N*-Methyl-D-aspartate (NMDA) receptors are inactivated by trypsin. *Brain Res.* **458**, 147–150.

Almers, W. (1978). Gating currents and charge movements in excitable membranes. *Rev. Physiol. Biochem. Pharmac.* **82**, 96–190.

Bell, R. A. and Joachim, F. G. (1976). Techniques for rearing laboratory colonies of tobacco hornworms and pink bollworms. *Ann. Ent. Soc. Am.* **69**, 365–373.

Bidmon, H.-J., Granger, N. A., Cherbas, P., Maròy, P. and Stumpf, W. E. (1991). Ecdysteroid receptors in the central nervous system of *Manduca sexta*: their changes in distribution and quantity during larval-pupal development. *J. Comp. Neurol.* **310**, 337–355.

Byerly, L. and Hagiwara, S. (1982). Calcium currents in internally perfused nerve cell bodies of *Lymnaea stagnalis*. *J. Physiol., Lond.* **322**, 503–528.

Byerly, L. and Hagiwara, S. (1988). Calcium channel diversity. In *Calcium and Ion Channel Modulation* (ed. A. D. Grinnel, D. Armstrong and M. B. Jackson), pp. 3–18. New York: Plenum Press.

Byerly, L. and Leung, H. T. (1988). Ionic currents of *Drosophila* neurons in embryonic cultures. *J. Neurosci.* **8**, 4379–4393.

Carlson, J. R. (1977). The imaginal ecdysis of the cricket (*Teleogryllus oceanicus*). I. Organization of the motor programs and roles of central and sensory control. *J. Comp. Physiol.* **115**, 299–317.

Christensen, B. N., Larmet, Y., Shimahara, T., Beadle, D. and Pichon, Y. (1988). Ionic currents in neurons isolated from embryonic cockroach (*Periplaneta americana*) brains. *J. Exp. Biol.* **135**, 193–214.

Connor, J. A. and Stevens, C. F. (1971a). Voltage clamp studies of a transient outward membrane current in gastropod neural somata. *J. Physiol., Lond.* **213**, 21–30.

Connor, J. A. and Stevens, C. F. (1971b). Prediction of repetitive firing behavior from voltage clamp data on an isolated neurone soma. *J. Physiol., Lond.* **213**, 31–53.

Copenhaver, P. F. and Truman, J. W. (1982). The role of eclosion hormone in the larval ecdyses of *Manduca sexta*. *J. Insect Physiol.* **28**, 695–701.

Curtis, A. T., Hori, M., Green, J. M., Wolfgang, W. J., Hiruma, K. and Riddiford, L. M. (1984). Ecdysteroid regulation of the onset of cuticular melanization in allatectomized and black mutant *Manduca sexta* larvae. *J. Insect Physiol.* **30**, 597–606.

Doroshenko, P. A., Kostyuk, P. G. and Martynyuk, A. E. (1982). Intracellular metabolism of adenosine 3′,5′-cyclic monophosphate and calcium inward current in perfused neurones of *Helix pomatia*. *Neuroscience* **7**, 2125–2134.

Eckert, R. and Chad, J. E. (1984). Inactivation of Ca channels. *Prog. Biophys. Mol. Biol.* **44**, 215–267.

Ewer, J., Gammie, S. C. and Truman, J. W. (1997). Control of insect ecdysis by a positive-feedback endocrine system: roles of eclosion hormone and ecdysis triggering hormone. *J. Exp. Biol.* **200**, 869–881.

Fox, A. P., Nowycky, M. C. and Tsien, R. W. (1987a). Kinetic and pharmacological properties distinguishing three types of calcium currents in chick sensory neurons. *J. Physiol., Lond.* **394**, 149–172.

Fox, A. P., Nowycky, M. C. and Tsien, R. W. (1987b). Single-channel recordings of three types of calcium channels in chick sensory neurons. *J. Physiol., Lond.* **394**, 173–200.

Gammie, S. C. and Truman, J. W. (1999). Eclosion hormone provides a link between ecdysis-triggering hormone and crustacean cardioactive peptide in the neuroendocrine cascade that controls ecdysis behavior. *J. Exp. Biol.* **202**, 343–352.

Grolleau, F. and Lapied, B. (1995). Separation and identification of multiple potassium currents regulating the pacemaker activity of insect neurosecretory cells (DUM neurons). *J. Neurophysiol.* **73**, 160–171.

Hagiwara, S. and Byerly, L. (1981). Calcium channel. *Annu. Rev. Neurosci.* **4**, 69–125.

Hagiwara, S. and Ohmori, H. (1982). Studies of calcium channels in rat clonal pituitary cells with patch electrode voltage clamp. *J. Physiol., Lond.* **331**, 231–252.

Hamill, O. P., Marty, A., Neher, E., Sakmann, B. and Sigworth, F. J. (1981). Improved patch-clamp techniques for high-resolution current recording from cells and cell-free membrane patches. *Pflügers Arch.* **391**, 85–100.

Hayashi, J. H. and Levine, R. B. (1992). Calcium and potassium currents in leg motoneurons during postembryonic development in the hawkmoth *Manduca sexta*. *J. Exp. Biol.* **171**, 15–42.

Hess, P., Lansman, J. B. and Tsien, R. W. (1986). Voltage and concentration dependence of single channel current in ventricular heart cells. *J. Gen. Physiol.* **88**, 293–319.

Hewes, R. S. (1993). The regulation and distribution of eclosion

hormone release in the tobacco hornworm, *Manduca sexta*. PhD thesis, Department of Zoology, University of Washington, Seattle, WA, USA.

Hewes, R. S. and Truman, J. W. (1991). The roles of central and peripheral eclosion hormone release in the control of ecdysis behavior in *Manduca sexta. J. Comp. Physiol*. A **168**, 697–707.

Hewes, R. S. and Truman, J. W. (1994). Steroid regulation of excitability in identified insect neurosecretory cells. *J. Neurosci.* **14**, 1812–1819.

Heyer, C. B. and Lux, H. D. (1976). Control of the delayed outward potassium currents in bursting pace-maker neurones of the snail, *Helix pomatia. J. Physiol., Lond.* **262**, 349–382.

Hille, B. (1992). *Ion Channels of Excitable Membranes*. Sunderland, MA: Sinauer.

Kloppenburg, P. and Hörner, M. (1998). Voltage-activated currents in identified giant interneurons isolated from adult crickets *Gryllus bimaculatus*. *J. Exp. Biol.* **201**, 2529–2541.

Latorre, R., Oberhauser, A., Labarca, P. and Alvarez, O. (1989). Varieties of calcium-activated potassium channels. *Annu. Rev. Physiol*. **51**, 385–399.

Leung, H. T., Branton, W. D., Phillips, H. S., Jan, L. and Byerly, L. (1989). Spider toxins selectively block calcium currents in *Drosophila*. *Neuron* **3**, 767–772.

Ma, M. and Koester, J. (1996). The role of K^+ currents in frequency-dependent spike broadening in *Aplysia* R20 neurons: a dynamic-clamp analysis. *J. Neurosci*. **16**, 4089–4101.

Marty, A. and Neher, E. (1983). Tight-seal whole-cell recording. In *Single-Channel Recording* (ed. B. Sakmann and E. Neher), pp. 107–122. New York: Plenum Press.

Mills, J. D. and Pitman, R. M. (1997). Electrical properties of a cockroach motor neuron soma depend on different characteristics of individual Ca components. *J. Neurophysiol.* **78**, 2455–2466.

Miyazaki, S. (1980). The ionic mechanism of action potentials in neurosecretory cells and non-neurosecretory cells of the silkworm. *J. Comp. Physiol*. **140**, 43–52.

Moody, W. J. and Bosma, M. M. (1985). Hormone-induced loss of surface membrane during maturation of starfish oocytes: Differential effects on potassium and calcium channels. *Dev. Biol*. **112**, 396–404.

Nightingale, W. D. and Pitman, R. M. (1989). Ionic currents in the soma of an identified cockroach motoneurone recorded under voltage-clamp. *Comp. Biochem. Physiol.* A **93**, 85–93.

O'Brien, M. A. and Taghert, P. H. (1998). A peritracheal neuropeptide system in insects: release of myomodulin-like peptides at ecdysis. *J. Exp. Biol.* **201**, 193–209.

Ohmori, H. and Yoshii, M. (1977). Surface potential reflected in both gating and permeation mechanisms of sodium and calcium channels of the tunicate egg cell membrane. *J. Physiol., Lond.* **267**, 429–463.

Reynolds, S. E. (1980). Integration of behavior and physiology in ecdysis. *Adv. Insect Physiol*. **15**, 475–595.

Richard, S., Tiaho, F., Charnet, P., Nargeot, J. and Nerbonne, J. M. (1990). Two pathways for Ca^{2+} channel gating differentially modulated by physiological stimuli. *Am. J. Physiol*. **258**, H1872–H1881.

Riddiford, L. M., Hewes, R. S. and Truman, J. W. (1994). Dynamics and metamorphosis of an identifiable peptidergic neuron in an insect. *J. Neurobiol*. **25**, 819–830.

Riddiford, L. M. and Truman, J. W. (1978). Biochemistry of insect hormones and insect growth regulators. In *Biochemistry of Insects* (ed. M. Rockstein), pp. 307–357. New York: Academic Press.

Sachs, F. and Auerbach, A. (1983). Single-channel electrophysiology: Use of the patch clamp. *Meth. Enzymol*. **103**, 147–176.

Simoncini, L. and Moody, W. J. (1991). Dependence of Ca^{2+} and K^+ current development on RNA and protein synthesis in muscle lineage cells of the ascidian *Boltenia villosa*. *J. Neurosci*. **11**, 1413–1420.

Singh, S. and Wu, C.-F. (1989). Complete separation of four potassium currents in *Drosophila*. *Neuron* **2**, 1325–1329.

Solc, C. K. and Aldrich, R. W. (1988). Voltage-gated potassium channels in larval CNS neurons of *Drosophila. J. Neurosci*. **8**, 2556–2570.

Thomas, M. V. (1984). Voltage-clamp analysis of a calcium-mediated potassium conductance in cockroach (*Periplaneta americana*) central neurons. *J. Physiol., Lond.* **350**, 159–178.

Thompson, S. (1982). Aminopyridine block of transient potassium current. *J. Gen. Physiol*. **80**, 1–18.

Trifaró, J. M. and Poisner, A. M. (1985). Electrophysiological properties of secretory cells: an overview. In *The Electrophysiology of the Secretory Cell* (ed. A. M. Poisner and J. M. Trifaró), pp. 269–302. New York: Elsevier.

Trimmer, B. A. and Weeks, J. C. (1989). Effects of nicotinic and muscarinic agents on an identified motoneurone and its direct afferent inputs in larval *Manduca sexta. J. Exp. Biol.* **144**, 303–337.

Truman, J. W. and Copenhaver, P. F. (1989). The larval eclosion hormone neurones in *Manduca sexta*: identification of the brain-proctodeal neurosecretory system. *J. Exp. Biol*. **147**, 457–470.

Truman, J. W., Rountree, D. B., Reiss, S. E. and Schwartz, L. M. (1983). Ecdysteroids regulate the release and action of eclosion hormone in the tobacco hornworm, *Manduca sexta* (L.). *J. Insect Physiol.* **29**, 895–900.

Tsunoda, S. and Salkoff, L. (1995). Genetic analysis of *Drosophila* neurons: *Shal*, *Shaw* and *Shab* encode most embryonic potassium currents. *J. Neurosci*. **15**, 1741–1754.

Žitňan, D., Kingan, T. G., Hermesman, J. L. and Adams, M. E. (1996). Identification of ecdysis-triggering hormone from an epitracheal endocrine system. *Science* **271**, 88–91.